Tunability of the optical properties in the Y6(W,Mo)(O,N)12 system

François Cheviré, Frédéric Clabau, Olivier Larcher, Emmanuelle Orhan, Franck Tessier, Roger Marchand

Graphical Abstract

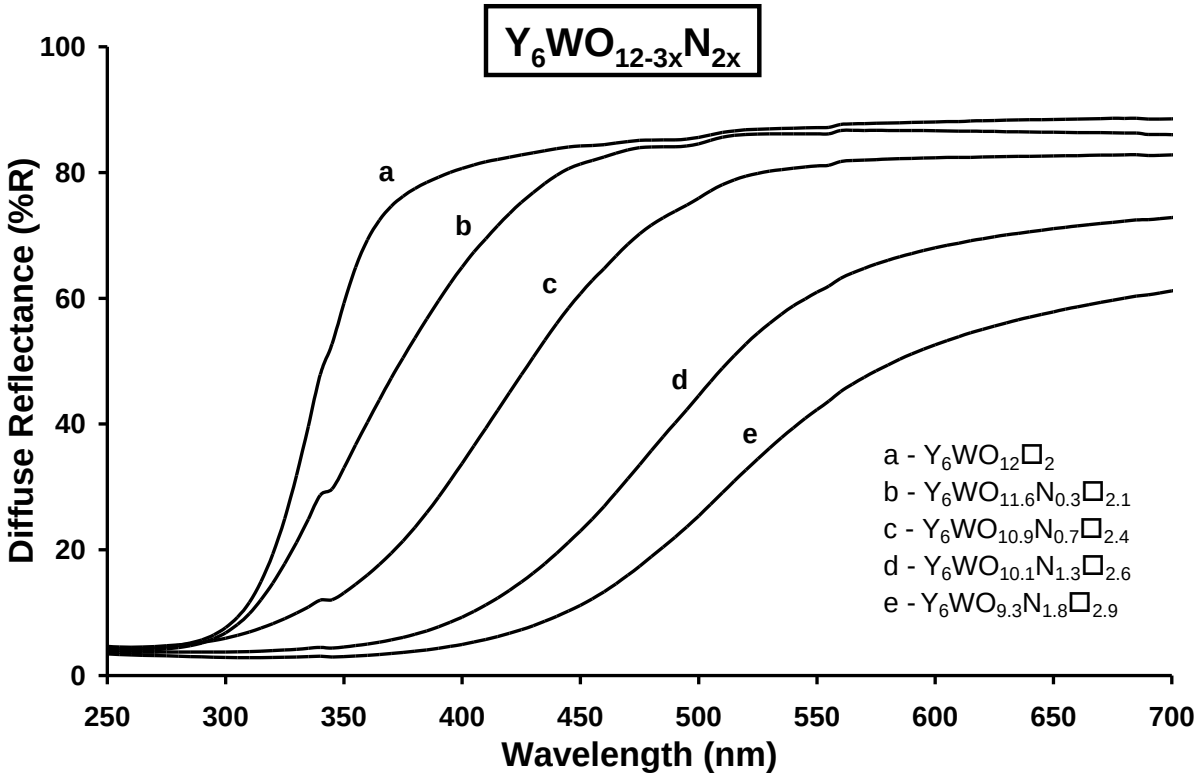

Tunability of the optical properties in the $Y_6(W,Mo)(O,N)_{12}$ system.

Cheviré François[a], Clabau Frédéric[a], Larcher Olivier[a], Orhan Emmanuelle[b], Tessier Franck[a]*, Marchand Roger[a].

a. UMR CNRS 6226 "Sciences Chimiques de Rennes" – Equipe "Verres et Céramiques" – Groupe Matériaux Nitrures - Université de Rennes 1 - F-35042 Rennes cedex, France

b. Laboratoire Science des Procédés Céramiques et Traitements de Surface, UMR CNRS 6638, Université de Limoges, 123 av. Albert Thomas, 87060 Limoges Cedex, France.

* Phone: +33 2 23 23 62 56 ; Fax: +33 2 23 23 56 83 ; *Franck.Tessier@univ-rennes1.fr

Keywords

Rare earth tungstates, solid solution, optical properties, UV absorbers

Abstract

New fluorite-type solid solution domains have been evidenced in the system $Y_6(W,Mo)(O,N)_{12}$ using precursors prepared by the amorphous citrate route. The oxynitrides as well as the low temperature oxides (600°C) crystallize in a cubic-type symmetry while the oxides annealed above 1200°C exhibit a rhombohedral symmetry. Either cationic (W/Mo) or anionic (O/N) substitutions bring the possibility to tune the optical absorption of the yttrium tungstate Y_6WO_{12}, which potential as inorganic UV absorbers is discussed.

1. Introduction

Over the past years, the interest in ternary metal oxynitrides as pigments has been considerable because they exhibit bright colors and are free of toxic heavy metals [1-5]. For instance, starting from the defect fluorite-type tungstates $R_{14}WO_{33}$ and R_6WO_{12} (R = La → Lu and Y) - that could be also respectively formulated $A_4X_{7.33}\square_{0.67}$ and $A_4X_{6.86}\square_{1.14}$ (A for cations and X for anions) - Diot et al. have evidenced new oxynitride solid solution domains between the starting oxide and the limit formulation $A_4X_6\square_2$ [6]. This work has shown the possibility to tune selectively the absorption of the pigments by controlling the nitrogen content in the oxynitrides which exhibit a wide range of color from pale yellow to brown and kaki respectively for the nitrogen-rich products. The following compositions - $Y_6WO_{9.1}N_{1.9}\square_{3.0}$, $Sm_6WO_{8.3}N_{2.5}\square_{3.2}$ and $Sm_{14}W_4O_{23.4}N_{6.4}\square_{6.2}$ - were of interest as new yellow pigment able to compete with $BiVO_4$. Using the same concept of tunability of the optical absorption with the chemical composition in order to answer specific needs, we have recently reported the optical properties of fluorite-type compositions within the Y_6WO_{12}-CeO_2 solid solution and have studied their potential as inorganic UV absorber materials [7]. Keeping starting from the tungstate Y_6WO_{12}, here we have investigated the influence of both cationic and anionic substitutions on the optical properties through the study of two fluorite-type solid solutions: $Y_6(W_{1-x}Mo_x)O_{12}$ and $Y_6W(O_{12-3/2x}N_x)$.

2. Experimental

2.1. Preparation

Oxide precursors were synthesized by the amorphous citrate route as described in previous works [7, 8]. Y_2O_3 (99.99%), H_2WO_4 (99%) and MoO_3 (99%) were used as

the starting materials and $C_6H_8O_7$ (> 99%) as the chelating agent. Oxynitride powders were prepared by annealing the corresponding oxide precursors under flowing ammonia using the nitridation setup detailed elsewhere [4, 8].

2.2. Characterization

Powders were analyzed by X-ray diffraction (Philips PW3710) at room temperature using CuK_α radiation. Nitrogen and oxygen contents were determined with a LECO TC-436 analyzer using the inert gas fusion method. Diffuse reflectance spectra were collected using a Varian Cary 100 Scan spectrometer equipped with the integrating sphere Labsphere (DRC-CA-30I) and the optical gap was then determined using the theory of Kubelka-Munk [9].

2.3. Quantum mechanics

Calculations have been performed on the Y_6WO_{12} unit cell in the framework of the density functional theory (DFT) with the CRYSTAL06 code [10]. Becke's three-parameter hybrid nonlocal exchange functional [11] combined with the Lee-Yang-Parr gradient corrected correlation functional, B3LYP [12], has been used. The standard B3LYP hybrid method has been extensively used for molecules and also provides an accurate description of crystalline structures in regard to bond lengths, binding energies, and band gap values [13, 14]. Pseudopotentials have been used to describe the cores of W [15] and Y [16] atomic centers while the all electrons basis set 6-31G* described the oxygen atoms. The k-points sampling was chosen to be 40 points in the irreducible part of the Brillouin zone.

3. Results and Discussion

3.1. Y_6WO_{12}

The symmetry of the tungstates R_6WO_{12} depends on the rare earth elements: cubic or pseudo-cubic from La to Pr, pseudo-tetragonal from Nd to Gd, and rhombohedral from Tb to Lu and for Y [17]. The latter compounds show a structural analogy with the mixed-valent binary oxide Pr_7O_{12} [18-20] as well as the ternary oxide Y_6UO_{12} [21]. Yttrium based-system was preferentially studied because of the absence of localized 4f-4f transitions which could induce parasitic absorption bands. The crystal structure was refined for Y_6WO_{12} by Diot et al. and described as yttrium being sevenfold coordinated in a monocapped trigonal prism while the tungsten is sixfold coordinated by oxygen atoms forming a regular octaedra [22]. As reported in the literature for Y_6WO_{12} [23, 24], a phase transition from rhombohedral to cubic occurs at 1765 ± 25°C. Above this temperature, the unit cell corresponds to a fluorite and the compound can be formulated $Y_{3.43}W_{0.57}O_{6.86}\square_{1.14}$. A random distribution on both the cationic and anionic sub-networks has to be considered which means that there is no more oxygen/vacancies ordering and that yttrium and tungsten atoms occupy the same crystallographic site in spite of their very different ionic radii, 0.96 Å and 0.71 Å respectively in 7-fold coordination [25]. The average coordination for the cations is then 6.86; however the oxygen/vacancies disorder and the cubic symmetry let think to an effective coordination of 8 that is relatively large for Y^{3+} and even more for W^{6+}. Recently, Yoshimura et al. have shown that the cubic Y_6WO_{12} can be obtained and stabilized as a metastable phase at low temperature (600°C) using a complexation-calcination route. By heating above 1000-1200°C, the symmetry changes to the stable rhombohedral phase [26].

DFT calculations carried out on the rhombohedral form of Y_6WO_{12} and illustrated on Fig. 1 by the density of states (DOS) curves indicate that the VB ↔ CB electronic transitions are of the 2*p*(O) ↔ 5*d*(W) type. The calculated energy gap corresponding to the minimal transition is 4.04 eV in very good agreement with the one obtained by diffuse reflectance : 3.91 eV. This energy depends strongly on the W-O distances in the structure, the shorter the distance, the greater the gap energy. The gap between the 5*d*(W) and 4*d*(Y) bands is large, i.e. 3.49 eV, so the yttrium orbitals are not directly involved in the optical band gap.

Before any further discussion, let us make some remarks at the level of the simple atomic bond. From this simple DOS figure, it is easy to understand that the interaction of an anion less electronegative than the oxygen with the tungsten at equivalent distances will result in levels in the valence band above the levels resulting from the W-O interaction. It is the case of nitrogen which introduction into the structure causes a reduction of the VB ↔ CB band gap. The same holds true for the substitution of tungsten by a more electronegative cation as for example molybdenum whose interaction with oxygen will tend to close the band gap. However, the substitution of the yttrium by another trivalent cation should not influence the bandgap value.

3.1. $Y_6WO_{12-3x}N_{2x}$

Here, low nitrogen contents were investigated in the way to prepared white or pale yellow compositions that display an absorption edge located around 400 nm (3.1 eV) giving them potential interest as inorganic UV absorbers. The oxide precursor used for the ammonolysis experiments is the metastable cubic phase obtained by the citrate route which has been discussed above. As mentioned in literature [3, 8], the use of such

precursors improves widely the reactivity of the oxide powders with ammonia. The experimental data are gathered in Table I and the diffuse reflectance spectra of the nitrided compositions shown in Figure 2A.

The nitridation results in a decrease of the diffuse reflectance maximum intensity and also in a continuous red shift of the absorption edge from 340 nm to about 525 nm. By adjusting the amount of nitrogen introduced into the yttrium tungstate structure, it becomes possible to synthesize an oxynitride composition that exhibits an absorption edge located at 400 nm, i.e. 3.1 eV. However, the spectral selectivities of the nitrided compositions appear to be too low to make them suitable for any UV absorption applications. Figure 2B displays the evolution of the bandgap vs. nitrogen content in the nitrided compositions. The bandgap tends to decrease linearly until the nitrogen content of x = 1 then the curve deviates to follow an asymptote around 2.5 eV that corresponds to a yellow color. Actually, no orange coloration of the powders was observed in this system.

3.3. $Y_6W_{1-x}Mo_xO_{12}$

As observed in the case of pure yttrium tungstate Y_6WO_{12}, the XRD patterns of the Mo-substituted products obtained by the amorphous citrate method at 600°C reveal a cubic symmetry while the rhombohedral symmetry is observed for the samples heated up to 1200°C. The absorption edges of the former phases are much more spread out that the ones of the latter (Fig. 3A). The calcination temperature (crystallinity) as well as the symmetry can give rise to such straightening of the absorption edges. First, the conduction band has mainly a metallic character, i.e. 5*d*(W) and 4*d*(Mo) orbitals; Secondly, the coordination sphere of the transition metal in the cubic phase is less regular and larger (cubic site with oxygen vacancies) than the regular octahedra in the

rhombohedral phase; So as the electronic band structure is very sensitive to the interatomic distances, the VB ↔ CB electronic transitions should be more defined for the rhombohedral phases than the cubic ones. This could explain the better absorption behavior of the rhombohedral phases. In addition, as molybdenum is more electronegative than tungsten, the energy level of the 4*d*(Mo) orbitals is lower than that of the 5*d*(W) orbitals. Consequently, a progressive substitution of Mo for W induces a red shift of the absorption edge, from 3.65 eV (Y_6WO_{12}) to 2.80 eV (Y_6MoO_{12}) (Fig. 3). The non linear variation of the optical bandgap along the solid solution suggests that the 4*d*(Mo) and 5*d*(W) levels form two bands relatively distinct from each other [27]. Among the rhombohedral phases, the compositions corresponding to $0.3 < x < 0.5$ appear to be attractive materials for anti-UV purposes, as they show bandgap values close to 3.1 eV with very narrow spectral selectivities ($\Delta Eg \sim 0.4 – 0.5$ eV).

4. Conclusion

Using precursors prepared through the amorphous citrate route, the optical properties of new oxynitride and oxide fluorite-type solid compositions have been characterized within the system $Y_6(W,Mo)(O,N)_{12}$. While the oxynitride and oxide cubic-type phases show less interest as new anti-UV pigments, promising compositions have been isolated among the rhombohedral phases.

References

[1] Jansen M, Letschert H. P., Nature 404 (1995) 980-982.

[2] Guenther E., Jansen M., Mater. Res. Bull. 36 (2001) 1399-1405.

[3] Cheviré F., Tessier F., Marchand R., Eur. J. Inorg. 6 (2006) 1223-1230.

[4] Tessier F., Marchand R., J. Solid State Chem. 171 (2003) 143-151.

[5] Aguiar R., Logvinovich D., Weidenkaff A., Rachel A., Reller A., Ebbinghaus S.G., Dyes and Pigments 76 (2008) 70-75.

[6] Diot N., Larcher O., Marchand R., Kempf J.-Y., Macaudière P., J. Alloys Comp. 323 (2001) 45-48.

[7] Cheviré F., Muñoz F., Baker C.F., Tessier F., Larcher O., Boujday S., Colbeau-Justin C., Marchand R., J. solid State Chem. 179 (2006) 3184-3190.

[8] Cheviré F., Tessier R., Marchand R., Mater. Res. Bull. 39 (2004) 1091-1101.

[9] Kubelka D., Munk L., Teck Z.. Physik. 12 (1931) 593-601.

[10] Dovesi R., Saunders V.R., Roetti C., Orlando C., Zicovitch-Wilson C.M., Pascale F., Civarelli B., Doll K., Harrison N.M., Bush I.J., D'Arco P., Llunell M., CRYSTAL06 User's Manual, University of Torino, Torino (2006).

[11] Becke A.D, J. Chem. Phys. 98 (1993) 5648.

[12] Lee C.T., Yang W.T., Parr R.G, Phys. Rev. B 37 (1988) 785.

[13] Hu C.-H., Chong D.P., Encyclopedia of Computational Chemistry, Wiley: Chichester (1998).

[14] Muscat J., Wander A., Harrison N.M., Chem. Phys. Lett. 342 (2001) 397.

[15] Cora F., Patel A., Harrison N.M., Dovesi R., Catlow C.R.A., J. Am. Chem. Soc. 118 (1996) 12174

[16] Gennard S., Cora F., 2000, unpublished data.

[17] McCarthy G.J., Fisher R.D., Johnson Jr. G.G., Gooden C.E., in: National Bureau ST. Special Publication 364, Solid State Chemistry, Proceedings of the 5th Materials Research Symposium (1972) 397.

[18] Ray S.P., Cox D.E., J. Solid State Chem. 15 (1975) 333.

[19] Von Dreele R.B., Eyring L., Bowman L., Yarnell J.L., Acta Crystallogr. B31 (1975) 971.

[20] Kang Z.C., Eyring L., J. solid State Chem. 75 (1988) 52.

[21] Bartram S.F., Inorg. Chem. 5 (1966) 749.

[22] Diot N., Bénard-Rocherullé P., Marchand R., Powder Diffraction 15 (2000) 220-226.

[23] Borschart H.J., Inorg. Chem. 2 (1963) 170-173.

[24] Kuribayashi K., Yoshimura M., Otha T., Sata T., J. Am. Ceram. Soc. 63 (1980) 644-646.

[25] Shannon R.D., Acta Cryst. A32 (1976) 751-767.

[26] Yoshimura M., Ma J., Kakihana M., J. Amer. Ceram. Soc. 81 (1998) 2721-2724.

[27] Larcher O., Thesis n°2259 (2001) Université de Rennes 1, France.

Table I: Experimental and optical data for the $Y_6(W,Mo)(O,N)_{12}$ system.

Thermal threatment	Chemical composition	%wt(N)	Eg (eV)	ΔEg (eV)	Color
	Oxynitride phases				
500°C/NH_3/5h	$Y_6WO_{11.6}N_{0.3}\square_{2.1}$	0.4	3.76	-	white
550°C/NH_3/5h	$Y_6WO_{10.9}N_{0.7}\square_{2.4}$	1.2	3.22	-	yellowish
600°C/NH_3/60h	$Y_6WO_{10.1}N_{1.3}\square_{2.6}$	2.0	2.75	-	yellow
800°C/NH_3/15h	$Y_6WO_{9.3}N_{1.8}\square_{2.9}$	2.9	2.56	-	mustard
	Cubic phases				
600°C/air/2h	Y_6WO_{12}	-	3.69	0.56	white
600°C/air/2h	$Y_6W_{0.9}Mo_{0.1}O_{12}$	-	3.75	1.05	cream
600°C/air/2h	$Y_6W_{0.7}Mo_{0.3}O_{12}$	-	3.28	0.82	pale yellow
600°C/air/2h	$Y_6W_{0.5}Mo_{0.5}O_{12}$	-	3.13	0.69	light yellow
600°C/air/2h	Y_6MoO_{12}	-	3.08	0.63	yellow
	Rhombohedral phases				
1200°C/air/2h	Y_6WO_{12}	-	3.91	0.53	white
1200°C/air/2h	$Y_6W_{0.9}Mo_{0.1}O_{12}$	-	3.33	0.65	cream
1200°C/air/2h	$Y_6W_{0.7}Mo_{0.3}O_{12}$	-	3.20	0.51	pale yellow
1200°C/air/2h	$Y_6W_{0.5}Mo_{0.5}O_{12}$	-	3.11	0.42	light yellow
1200°C/air/2h	Y_6MoO_{12}	-	3.00	0.35	yellow

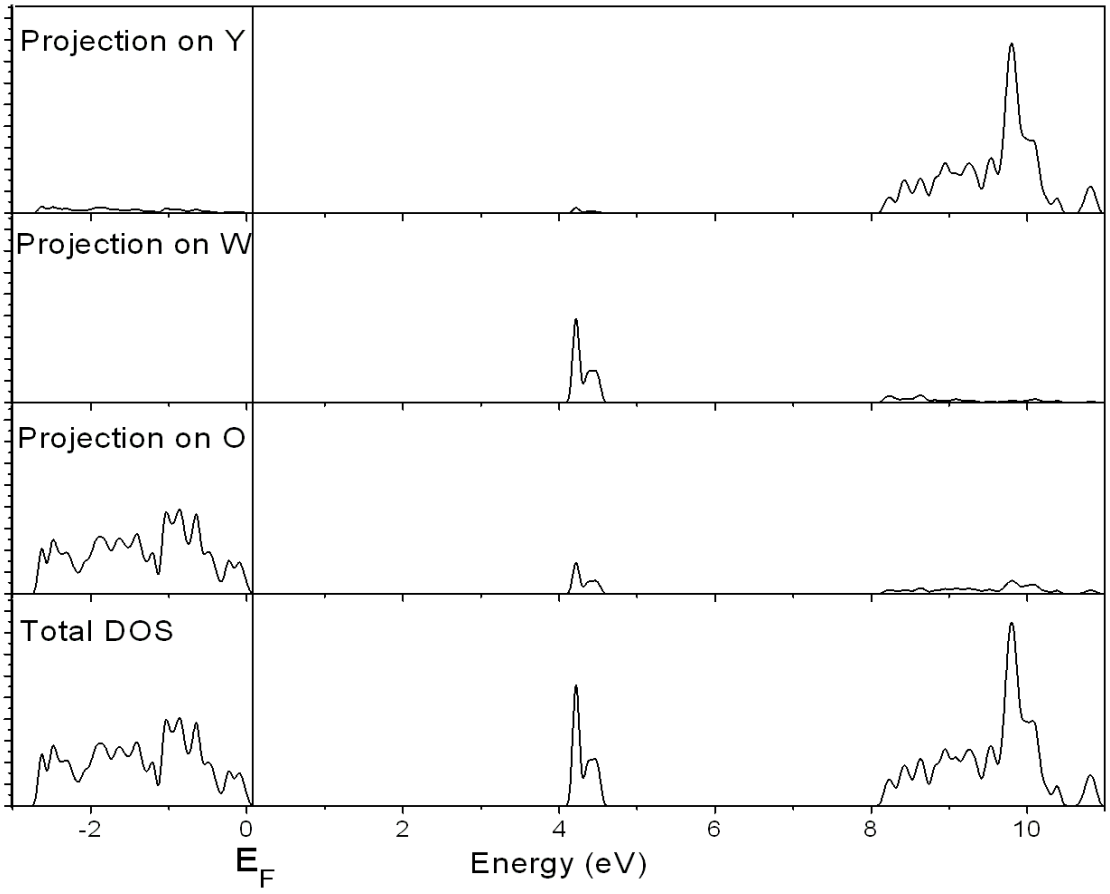

Figure 1: Total DOS and partial DOS projected on Y, W and O for the rhombohedral form of Y_6WO_{12}.

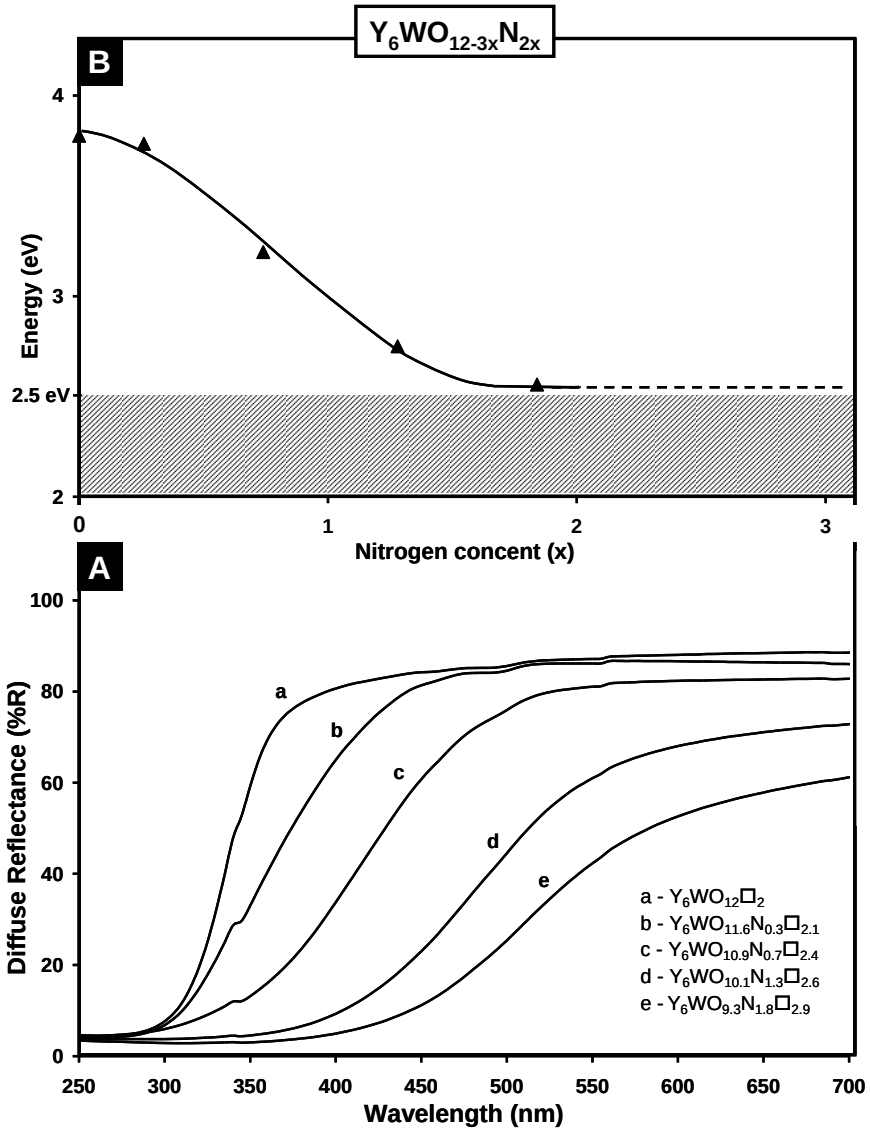

Figure 2 : Diffuse reflectance spectra and evolution of the optical gap vs. nitrogen content in the $Y_6WO_{12-3x}N_{2x}$ system.

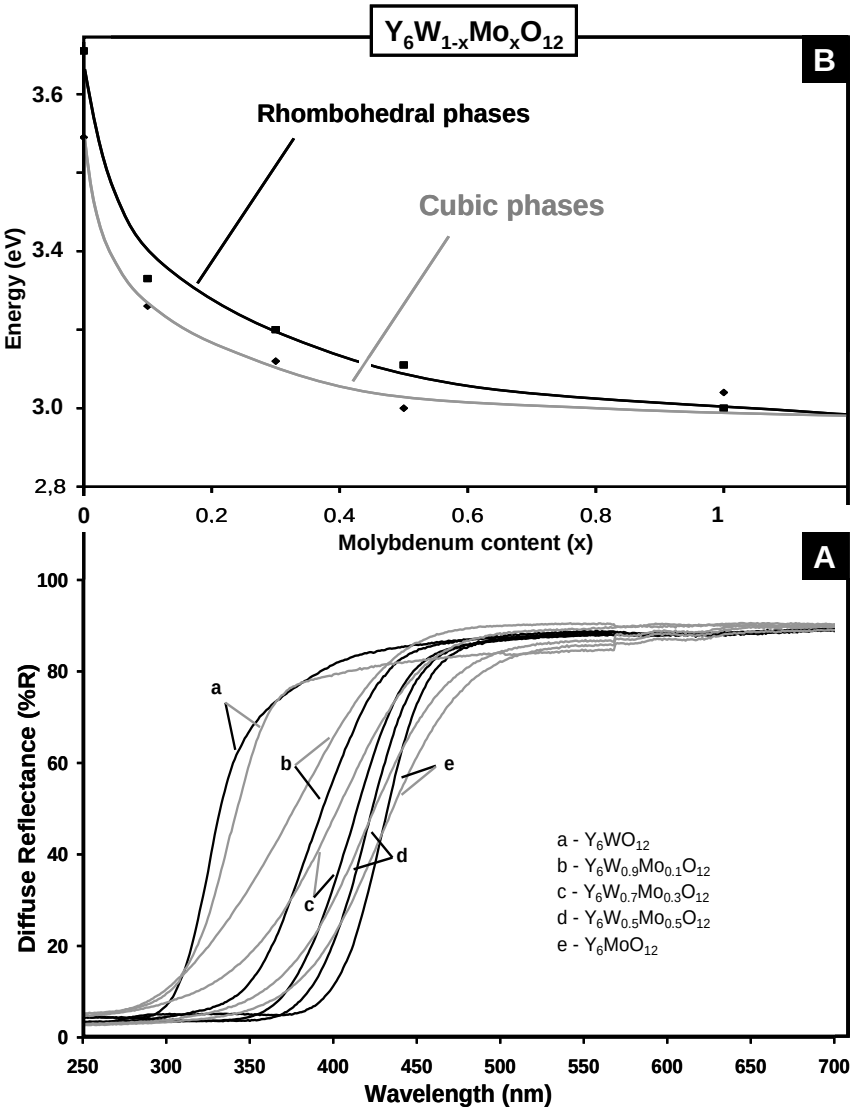

Figure 3 : Diffuse reflectance spectra and evolution of the optical gap vs. molybdenum content in the $Y_6W_{1-x}Mo_xO_{12}$ system.